Hindawi
Advances in Materials Science and Engineering
Volume 2019, Article ID 9520801, 9 pages
https://doi.org/10.1155/2019/9520801

Research Article

Prediction of Fatigue Life of Welded Joints Made of Fine-Grained Martensite-Bainitic S960QL Steel and Determination of Crack Origins

Tomasz Ślęzak

Military University of Technology, Faculty of Mechanical Engineering, Institute of Machine Building, Ul. Gen. W. Urbanowicza 2, 00-908 Warsaw, Poland

Correspondence should be addressed to Tomasz Ślęzak; tomasz.slezak@wat.edu.pl

Received 23 November 2018; Accepted 16 January 2019; Published 4 February 2019

Guest Editor: Dariusz Rozumek

Due to growing requirements connected with the utilization of advanced structures, nowadays the modern design processes are developed. One of the crucial issues considered in these processes is proper design of the joints against fatigue in order to fulfill a stated life of operation. In this study, the method of fatigue life prediction based on the criterion of permissible strain range in the notch root is presented. An engaged simplified model of fatigue life prediction was previously developed for mild and carbon steels. The evaluation made during the research has proven that this method can also be used for S960QL high-strength steel characterized by entirely different properties and structure. A considered theoretical model demonstrates satisfactory correlation with experimental data and safely describes the fatigue life of weldments. Furthermore, the predicted fatigue life of studied steel without welds shows great comparability with experimental data. The limit value of the strain range in the notch root was estimated. Below this value of strain, the fatigue life of welded joints is infinite, theoretically. Finally, the impact of the surface imperfections on the fatigue crack initiation was revealed. For paternal material, the origins of cracking were discovered at the places of nonmetallic scale particles. In welded joints, the fatigue cracks initiated at the whole length of the fusion line.

1. Introduction

Individual members of more complex structures are connected to each other in the nodes utilizing different techniques. Design requirements define whether this junction has to be demountable or permanent. The permanent manner of joining is obvious in the case of fabrication of the large and complex structures like bridges and other civil engineering constructions, heavy vehicle frames, pipeline systems, or cranes, exemplary. These types of structures require realization of numerous joints, and the welding is adequate to ensure an optimal efficiency of fabrication with proper finance outcome. The use of welding allows to reduce the thickness of structural elements decreasing the total weight of structure together with the number of employed consumables and finally influencing the reduction of fabrication costs. For these reasons, this connecting technique is widespread. Nevertheless, it has to be remembered that the junctions are the points weakening a structure and the most probable places of failure initiation. The above-mentioned structures are served in condition of alternating loads, and thus, the fatigue is predicted to be the major cause of rupture. This phenomenon is directly related to the changes of geometric shape, microstructure, and stress distribution occurring during the welding process. For these reasons, the highest probability where the crack origins occur is in the nearest vicinity of the weldments where numerous notches are discovered.

The complexity of this matter causes that different methods of prediction of the fatigue strength and fatigue life have hitherto been developed. The most popular is a division into three main approaches, namely, stress-, strain-, and energy-based.

The nominal stress approach is based on the assumption of overall elastic behaviour. The stress is computed in the considered section, and the effect of the macrogeometric

shape of the component, notches, and residual stresses are taken under account. Nevertheless, the local influence of the welded joints on the stress value is disregarded. For the reason of its simplicity, this method is the most widely used approach to design welded structures against fatigue [1–5].

In the case when nominal stresses cannot be determined with sufficient accuracy due to component complexity, the structural hot-spot stress approach should be engaged. This method takes into account all factors resulting in the increase of stress in the vicinity of the junction and works by extrapolating a reference stress value at the weld toes, with the stress gradient effect being accounted for through ad hoc compiled design curves [6, 7]. Two or three measures have to be realized at different distances from the weld toe in order to compute the value of stress in the weld toe. In the case of stress calculated on the plate surface, according to [1], it can be determined using extrapolation of the following equations:

$$\sigma_{\mathrm{hs}} = 1.67 \cdot \sigma_{0.4 \cdot t} - 0.67 \cdot \sigma_{1.0 \cdot t}, \tag{1}$$

$$\sigma_{\mathrm{hs}} = 2.52 \cdot \sigma_{0.4 \cdot t} - 2.24 \cdot \sigma_{0.9 \cdot t} + 0.72 \cdot \sigma_{1.4 \cdot t}. \tag{2}$$

The parameter t is the thickness of the considered component and $\sigma_{0.4 \cdot t}$ is the stress measured at the distance of $0.4\,t$ from the toe. The hot-spot stress approach is very often engaged during finite element analysis (FEA) of welded components. Moreover, novel numerical methods are being developed and, in this regard, distinctive or unique structure cases are considered [8–12]. Nevertheless, this approach is also insufficient in more complex cases due to the assumption of an elastic stress range with linear change. Therefore, the welded joints of these structures are designed against fatigue using the effective notch stress approach [13–19], which is the most advanced fatigue design method being recommended by IIW [1]. This approach is based on the statement that stresses in the notch bottom are determined in the weld toe/root rounded with a fictive radius of 1 mm or 0.5 mm when the thickness of welded component is larger than 5 mm or less, respectively. The idea behind this method is that the mechanical local behaviour of the material in the notch bottom is similar to the behaviour of an unnotched or slightly notched, miniaturized, and axially loaded specimen extracted from this area [20].

Described approaches can be successfully employed if the high-cycle fatigue strength in infinite life is taken under consideration. These instances are characterized by the presence of elastic stresses. Only the notch stress approach can be extended into a finite-life range where the plastic microstrains cause crack initiation and their development. The influence of plastic strains is more substantial in the range of a low-cycle fatigue obtained under high and very high loads.

This paper presents the results of research conducted on development of the simplified model of fatigue life prediction of welded joints utilized from a fine-grained high-strength structural steel. Initially, there is consideration of the matter of adoption of the existing description for HSS steel and its extension on welded joints. The experimental verification was carried out, and the fractographic studies of fatigue crack initiation were also presented.

2. Prediction of Fatigue Life

The description of fatigue behaviour in the low-cycle range has to consider the plastic component. This crucial reason causes that the strain- and energy-based approaches of fatigue life prediction are most suitable, in comparison with stress-based methods. The most common formula describes this relationship is the Morrow design rule (3):

$$\varepsilon_{\mathrm{a}} = \varepsilon_{\mathrm{ael}} + \varepsilon_{\mathrm{apl}} = \frac{\sigma_{\mathrm{f}}'}{E}\left(2N_{\mathrm{f}}\right)^{b} + \varepsilon_{\mathrm{f}}'\left(2N_{\mathrm{f}}\right)^{c}. \tag{3}$$

The above rule defines the dependence between strain amplitude ε_{a} divided into elastic and plastic components and pertinent fatigue life N_{f}. The coefficients σ_{f}' and $\varepsilon_{\mathrm{f}}'$ together with exponents b and c are determined during fatigue tests performed under the strain mode.

Alternative simplified solution of this problem was proposed by Manson [21]:

$$\Delta\varepsilon_{\mathrm{a}} = \Delta\varepsilon_{\mathrm{ael}} + \Delta\varepsilon_{\mathrm{apl}} = 3.5\frac{R_m}{E}\left(N_{\mathrm{f}}\right)^{-0.12} + \varepsilon_{\mathrm{fra}}^{0.6}\left(N_{\mathrm{f}}\right)^{-0.6}, \tag{4}$$

where only three material properties are used: ultimate strength R_m, yield modulus E, and ductility $\varepsilon_{\mathrm{fra}}$ defined as

$$\varepsilon_{\mathrm{fra}} \approx \ln\frac{100}{100 - Z}, \tag{5}$$

where Z is a percent area reduction.

Other version of relationships (3) and (4) is an equation developed by Langer [22]:

$$\varepsilon_{\mathrm{a}} = \varepsilon_{\mathrm{ael}} + \varepsilon_{\mathrm{apl}} = \frac{Z_{-1}}{E} + 0.25 \cdot \left(N_{\mathrm{f}}\right)^{-0.5} \ln\frac{100}{100 - Z}, \tag{6}$$

where Z_{-1} is the fatigue strength under fully reversed loading.

In the publication [23], authors proposed a new formula developed on the basis of relationships (3)–(6) with some modifications. Firstly, Z_{-1} is replaced in Equation (6) by $0.55R_m$ because according to [24] $Z_{-1} = \gamma R_m$ and $\gamma = 0.55$ is a coefficient depended on the material type. For steel, it is equal from 0.4 up to 0.55, and on the basis of results presented in [23], the maximum value has been chosen. Moreover, the influence of cycle asymmetry was also taken under account. According to [24], the plastic strain amplitude $\varepsilon_{\mathrm{apl}}$ was replaced by the medium plastic strain amplitude $\varepsilon_{\mathrm{mapl}}$:

$$\varepsilon_{\mathrm{mapl}} = \varepsilon_{\mathrm{apl}}\frac{1 + R}{1 - R}. \tag{7}$$

Considered relationships were developed and evaluated for carbon and mild steels with $R_m < 700$ MPa. In the case of high-strength steels that have another microstructure and strengthening mechanism, Z parameter should be replaced by $Z^x = 0.5Z + 15$ [24]. Moreover, in order to define the permissible strain range $\Delta\varepsilon_{\mathrm{per}}$ and the permissible fatigue life N_{per}, the partial factors of safety ψ_ε and ψ_N were imposed, defined in Equations (8). The first is related to $\Delta\varepsilon_{\mathrm{a}}$ and the second is related to N_{f}, respectively:

$$\psi_\varepsilon = \frac{\Delta\varepsilon_a}{\Delta\varepsilon_{per}}, \qquad \psi_N = \frac{N_f}{N_{per}}. \tag{8}$$

As a result, the following relationships describing $\Delta\varepsilon_{per}$ and N_{per} were obtained:

$$\Delta\varepsilon_{per} = \frac{2}{2\cdot\left(\psi_N\cdot N_f\right)^m + \left((1+R_\varepsilon)/(1-R_\varepsilon)\right)}\cdot \ln\frac{100}{100-Z^x} + \frac{1.1R_m}{E}, \tag{9}$$

$$N_{per} = \left(\frac{1}{\psi_\varepsilon\cdot\Delta\varepsilon_a - \left((1.1R_m)/E\right)}\cdot \ln\frac{100}{100-Z^x} - \frac{1+R_\varepsilon}{2\cdot\left(1-R_\varepsilon\right)}\right)^{1/m}. \tag{10}$$

2.1. Prediction of Low-Cycle Fatigue Life of Welded Joints. In order to describe predicted fatigue life of welded joints, the notch strain approach was proposed. Therefore, the value of elastic-plastic strain range in the notch root $\Delta\varepsilon_{notch}$ should be specified. In the considered case, the notch is localized at the fusion line of weld. The condition of low-cycle fatigue strength is fulfilled if

$$\Delta\varepsilon_{notch} \le \Delta\varepsilon_{per}, \tag{11}$$

which means that the strain should not exceed the limit value determined for the locally changed material at the notch. The strain range $\Delta\varepsilon_{notch}$ can be expressed by the product of strain concentration factor α_ε and the nominal strain range $\Delta\varepsilon_N$:

$$\Delta\varepsilon_{notch} = \alpha_\varepsilon\cdot\Delta\varepsilon_N. \tag{12}$$

According to [23], the strain concentration factor can be calculated using the following formula:

$$\alpha_\varepsilon = \frac{\alpha_k^{[2/(1+n)]}\cdot\overline{\Delta}\sigma_N^{[(1-n)/(1+n)]}}{\left(\alpha_k\cdot\overline{\Delta}\sigma_N\right)^{a\cdot(1-n)\cdot\left(1-\overline{\Delta}\sigma_N+\left(1/\sigma_k\right)\right)/(1+n)}}, \tag{13}$$

where α_k is the stress concentration factor (weld shape induced), n is the strain-hardening exponent, a is the constant (equal from 0 to 0.5), $\overline{\Delta}\sigma_N = \Delta\sigma_N/((1-R_\sigma)\cdot R_e)$ is the normalized range of nominal stresses, $\Delta\sigma_N$ is the nominal stress range, and R_σ is the loading stress ratio.

The range of nominal strain $\Delta\varepsilon_N$ was computed using the following dependence:

$$\Delta\varepsilon_N = \frac{\Delta\sigma_N}{E}. \tag{14}$$

In order to determine the dependence describing predicted fatigue life of welded joints and taking into account condition (11), equation (10) was modified. Hitherto strain was replaced by $\Delta\varepsilon_{notch}$, and two new factors of safety were considered, namely, ψ_{Ff} related to the uncertainty degree of the used theoretical model and ψ_{Mf} related to the sensitivity of the material on cracking connected with the accessibility to supervise the welded structure (15):

$$N_f = \left(\frac{1}{\psi_{Ff}\cdot\psi_{Mf}\cdot\Delta\varepsilon_{notch} - \left((1.1R_m)/E\right)}\cdot \ln\frac{100}{100-Z^x} - \frac{1+R_\varepsilon}{2\cdot\left(1-R_\varepsilon\right)}\right)^{1/m}. \tag{15}$$

3. Experimental Procedure

3.1. Materials. Experimental validation of the model of fatigue life prediction was carried out on fine-grained high-strength structural steel S960QL. The used material was in the form of sheet with a thickness of 6 mm. This steel is produced by liquid-quenching and tempering (Q&T) process which results in bainite-martensitic microstructure. The results obtained during chemical composition measurements and mechanical properties tests are presented in Tables 1 and 2.

The study of the chemical composition has been carried out using scanning electron microscopy equipped with an EDS spectrometer. Mechanical properties were determined on the basis of the results of tensile tests carried out according to [25].

3.2. Welded Joints. The fatigue tests were carried out using two types of butt joints, namely, I-shaped and V-shaped. The geometry of the connected parts before welding is shown in Figure 1.

The welds were made using MAG (metal active gas) welding with shielding gas containing 82% CO_2 and 18% Ar (EN ISO 14175–M21–ArC–18). Wire UNION X96 (EN ISO 16834–A–G Mn4Ni2,5CrMo) with a diameter of 1.2 mm was used to make the welds. The weld type presented in Figure 1(a) was made in a fully robotized way, in contrast to the second where the first run (root side) was made manually and only the second run (face side) using a mechanised method.

3.3. Fatigue Life Test Procedure. Fatigue tests were performed in terms of the low-cycle fatigue (LCF) and carried out for the paternal material and both types of welded joints. The tests were conducted using flat samples prepared on the basis of standard ASTM E606-4 [26]. Test samples were cut from a sheet with a nominal thickness of 6 mm, and their geometry is shown in Figure 2.

It was assumed that the fatigue tests will be performed on the material in the supply condition, which means that the surface of the test samples was not subjected to machining. The aim was to reflect as closely as possible the causes of fatigue crack initiation in real conditions.

Fatigue tests were carried out using an Instron 8808 hydraulic pulsator equipped with a dynamic extensometer. Two different gauges with the length of 25 mm and 50 mm were used during fatigue tests of the paternal material and welded joints, respectively. The tests were conducted in the strain mode controlled with the value of the total strain amplitude ε_a with a sinusoidal waveform. The values of amplitude ε_a fit in the range of 0.30% to 1.5% for the paternal material and from 0.15% to 0.40% for the joints. The value of the strain ratio R_ε of 0.1 and an average strain rate of $\dot{\varepsilon} = 10^{-2}\cdot s^{-1}$ were adopted. The failure criterion was a 25% decrease of maximum load.

Table 1: Chemical composition of S960QL steel.

	C	Si	Mn	Cr	Mo	Ni	Al	V	Cu
Own measurement	0.18	0.36	1.19	0.23	0.66	0.06	0.11	0.03	0.19
According to the certificate	0.18	0.28	1.13	0.22	0.67	0.08	0.08	0.03	0.18

Table 2: Mechanical properties of S960QL steel.

	E (MPa)	$R_{p0.2}$ (MPa)	R_m (MPa)	A (%)	Z (%)
Own measurement	2.20×10^5	974	1070	14.2	45.6
According to the certificate	—	997	1069	13.0	—

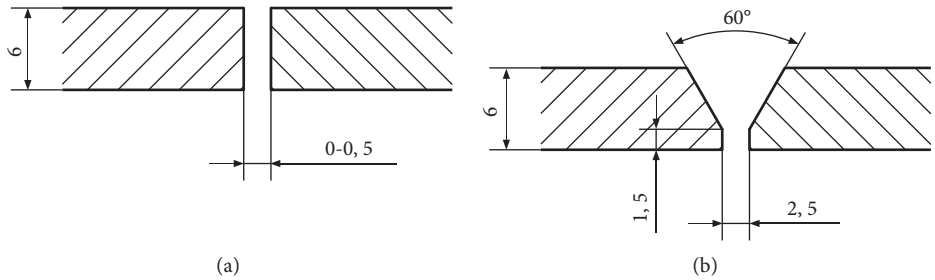

Figure 1: Geometry of welded elements prior to the implementation of joints: I-shaped (a) and V-joints (b).

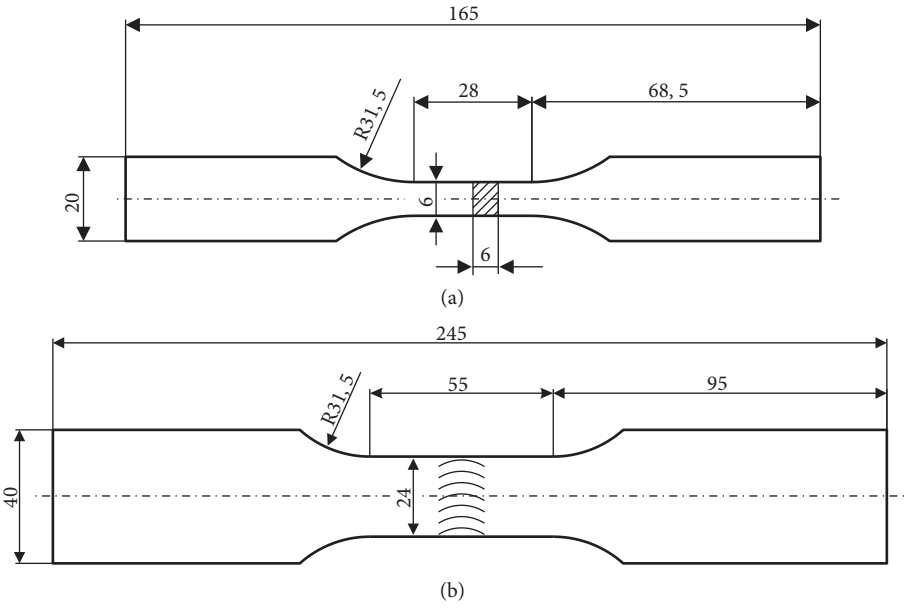

Figure 2: Dimensions of samples used in fatigue tests conducted on the paternal material (a) and welded joints (b).

4. Results and Discussion

4.1. Fatigue Test Results. In order to validate the developed theoretical model of fatigue life prediction, firstly, the fatigue tests were conducted on the paternal material—steel S960QL. Examination was carried out under six different total strain amplitudes: 0.30%, 0.40%, 0.50%, 0.75%, 1.0%, and 1.5%. Obtained results are shown in Table 3.

Based on these results and taking into account that the dependence $\sigma_a = f(\varepsilon_{apl})$ expressed by (16) in the log-log scale is similar to linear function, the hardening exponent n for examined steel was determined. Its value is equal to 0.0769:

$$\sigma_a = K' \cdot \left(\varepsilon_{apl}\right)^n. \quad (16)$$

Secondly, the fatigue tests on the welded joints were conducted. Examination was carried out under five different total strain amplitudes, namely, 0.15%, 0.20%, 0.25%, 0.30%, and 0.40%. Obtained results are shown in Table 4.

4.2. Comparison of the Fatigue Life Prediction Model with Experimental Results. At the beginning, the theoretical ε_{per}-N_{per} curve for S960QL steel was determined based on formula (10). In calculations, the values of parameters R_m, E,

Table 3: Results of fatigue tests for S960QL steel.

Load ε_a (%)	ε_{apl} (%)	ε_{ael} (%)	N_f (cycles)	σ_a (MPa)
0.30	0.0097	0.2903	11863	603
	0.0066	0.2934	10488	597
0.40	0.0669	0.3331	5731	680
0.50	0.1184	0.3816	1867	754
	0.1377	0.3623	1688	771
0.75	0.3178	0.4322	583	814
	0.3227	0.4273	612	811
1.00	0.5380	0.4620	272	834
	0.5400	0.4600	262	846
1.50	1.0080	0.4920	140	842

Table 4: Results of fatigue tests for welded joints of S960QL steel.

Load ε_a (%)	Joint type	ε_{apl} (%)	ε_{ael} (%)	N_f (cycles)	σ_a (MPa)
0.15	I	0.0027	0.1473	6858	306
	I	0.0013	0.1487	5195	309
	V	0.0012	0.1488	13851	290
	V	0.0012	0.1488	7036	311
0.20	I	0.0029	0.1971	3160	413
	I	0.0025	0.1975	2444	421
	V	0.0015	0.1985	1892	445
	V	0.0020	0.1980	1755	400
0.25	I	0.0026	0.2474	1298	536
	I	0.0025	0.2475	914	545
	I	0.0063	0.2437	1610	534
	V	0.0020	0.2480	1095	534
	V	0.0040	0.2460	1418	478
0.30	I	0.0087	0.2913	772	604
	I	0.0088	0.2912	969	610
	V	0.0074	0.2926	553	652
	V	0.0085	0.2915	699	624
0.40	I	0.0323	0.3677	268	740
	V	0.0425	0.3575	178	788
	V	0.0330	0.3670	274	713

and Z (to calculate Z^x) have been taken from Table 2 and $R_\varepsilon = 0.1$ from the experiment conditions. It is proposed to take a value of material exponent $m = 0.6$ [24]. The factor of safety was assumed to be equal to 1.0 because this dependence describes theoretical relation between strain and fatigue life. The final results are presented on the graph (Figure 3).

In Figure 3, two curves are presented. The first curve was plotted on the basis of the developed model of permissible fatigue life expressed by equation (10). The second curve was obtained from registered experimental data and expressed by the Morrow curve (3). Additionally, the results of fatigue life for tested samples are placed. The presented graphs show a proper correlation between the adopted theoretical model for describing the fatigue life of the S960QL steel with the results obtained in the experimental way.

In order to establish the N_f function concerning the welded joints of S960QL steel (15), determination of stress concentration factor α_k is crucial. Three methods were considered, namely, Jewdokimow's, Lawrance's, and Ushirokawa–Nakayama's, and the first was recommended as

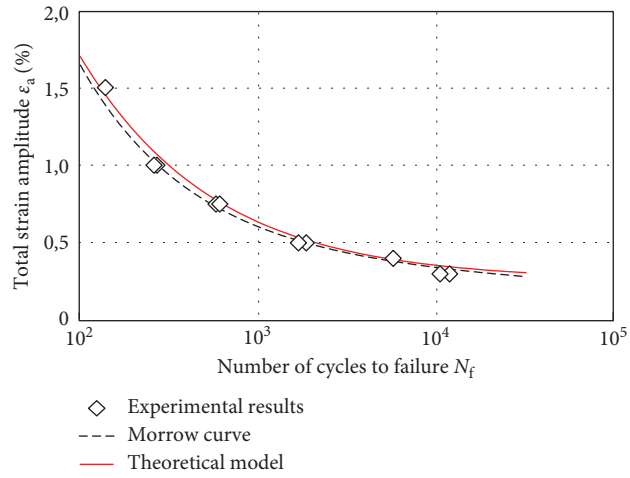

Figure 3: Comparison of the developed theoretical model with experimental results.

the most severe [27]. Measurements of the radius in the notch root ρ were performed which reached the value of 0.5–1.1 mm. Because the measurements were made locally in random cross-sections, $\rho = 0.5$ mm was taken under further consideration. Then, the values of α_k factor have equalled approximately 1.93 in the case of I-shaped weld and from 1.61 up to 1.81 for V-shaped weld, and the worst values of $\alpha_k = 1.93$ and $\alpha_k = 1.81$ were adopted, respectively. Moreover, the stress range $\Delta\sigma_N$ was taken as a double value of strain amplitude σ_a (Table 4) and n exponent from equation (16). Loading stress ratio R_σ was determined individually in each test taking into account the maximum and minimum values of recorded stresses from the middle cycle of the fatigue life. Material constant $a = 0.5$ was taken. The strain range $\Delta\varepsilon_N$ was calculated according to equation (14). Obtained results are presented in Table 5 and shown on the plot (Figure 4).

On the basis of the developed plot (Figure 4), it can be stated that the elaborated theoretical model of prediction of the fatigue life describes it in a simple and safe way. Moreover, the assumed fatigue strength criterion based on the maximum strain in the notch root was proper for the case of welded joints made of high-strength steel. The analysis made on the basis of results obtained for $N_f > 1000$ cycles leads to the conclusion that influence of R_ε in this range is negligible. For presented results, the most important advantage is that predicted values are slighter than the results obtained during fatigue tests. Furthermore, final equation (17) describing the dependence of the predicted fatigue life of S960QL steel-welded joints N_f versus the strain range in the notch root $\Delta\varepsilon_{notch}$ was elaborated:

$$N_f = \left(\frac{0.475}{1.725 \cdot \Delta\varepsilon_{notch} - 5.36 \cdot 10^{-3}} - 0.61\right)^{1.67}. \quad (17)$$

The experimental research results and the theoretical values are characterized by noticeable good correlation particularly under lower values of strain $\Delta\varepsilon_{notch}$. Determined values of strain bring about the fatigue life no lower than 5000 cycles. It can be probably caused by the significant reduction or even partial cessation of plastic strains in the

Table 5: Results of calculations of the strain range $\Delta\varepsilon_{notch}$.

Load ε_a (%)	Joint type	$\Delta\sigma_N$ (MPa)	R_σ (−)	$\overline{\Delta}\sigma_N$ (−)	α_ε (−)	$\Delta\varepsilon_N$ (%)	$\Delta\varepsilon_{notch}$ (%)
0.15	I	611	−0.02	0.616	2.09	0.278	0.58
	I	618	+0.03	0.651	2.16	0.281	0.61
	V	579	−0.19	0.500	1.74	0.264	0.46
	V	622	+0.33	0.953	2.51	0.283	0.71
0.20	I	826	−0.09	0.780	2.41	0.376	0.91
	I	841	−0.11	0.778	2.40	0.383	0.92
	V	890	−0.135	0.805	2.22	0.405	0.90
	V	800	+0.13	0.944	2.49	0.364	0.91
0.25	I	1072	−0.02	1.082	3.16	0.488	1.54
	I	1090	−0.21	0.925	2.74	0.496	1.36
	I	1067	−0.16	0.944	2.79	0.486	1.35
	V	1068	−0.17	0.937	2.48	0.486	1.20
	V	956	−0.14	0.861	2.32	0.435	1.01
0.30	I	1207	−0.24	0.999	2.93	0.550	1.61
	I	1219	−0.40	0.894	2.66	0.555	1.48
	V	1302	−0.47	0.909	2.42	0.593	1.43
	V	1248	−0.41	0.909	2.42	0.568	1.37
0.40	I	1479	−0.63	0.932	2.75	0.00673	1.85
	V	1425	−0.58	0.926	2.45	0.00649	1.59
	V	1576	−0.77	0.914	2.43	0.00718	1.74

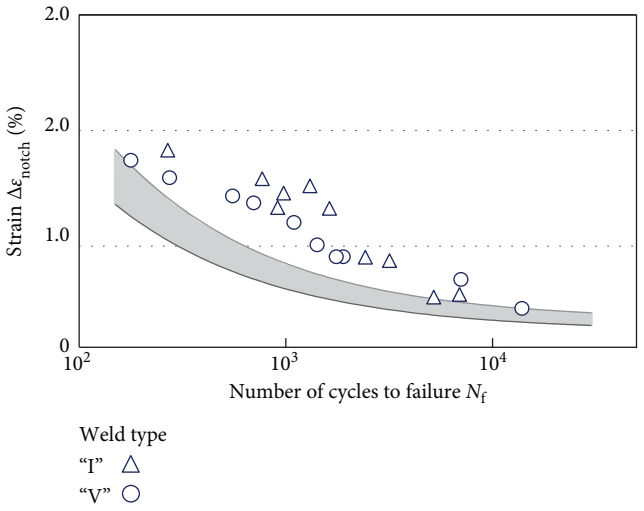

Figure 4: Comparison of the results obtained for the developed theoretical model of fatigue life prediction with experimental data. Grey area is the range of predicted fatigue life defined by equation (14) and obtained for different values of safety factors.

notch root. However, a limit value of the strain range in the notch root $\Delta\varepsilon_{notch}$ for which an unlimited fatigue life takes place can be determined taking into account the issue $N_f \longrightarrow \infty$:

$$\Delta\varepsilon_{notch} = \lim_{N_f \longrightarrow \infty} \left[\frac{1}{\psi_{Ff} \cdot \psi_{Mf}} \left(\frac{1}{(N_f)^m + ((1+R_\varepsilon)/(2\cdot(1-R_\varepsilon)))} \cdot \ln \frac{100}{100 - Z^x} + \frac{1.1R_m}{E} \right) \right]. \tag{18}$$

The limit value of $\Delta\varepsilon_{notch}$ calculated using formula (18) equals $3.11 \cdot 10^{-3}$. The predicted value of stress range $\Delta\sigma$ was determined using this strain, specific for S960QL steel, and it amounts to at least 300 MPa. This value was computed under the statement that the maximum strain concentration factor α_ε equals 2.2 and was determined for $\varepsilon_a = 1.5 \cdot 10^{-3}$.

4.3. Fractographic Investigation on Fatigue Crack Initiation. The studies of fatigue crack surfaces were conducted using the scanning electron microscope JEOL JSM-6610, and the observations were realized by SE (secondary electrons) and BSE (backscattered electrons) detectors. Both the paternal material and welded joint samples are explored (Figures 5 and 6).

In Figures 5(a) and 5(b) are presented the exemplary fatigue fractures resulting from fatigue tests conducted at the total strain amplitude $\varepsilon_a = 0.3\%$ and 1.5%, respectively. Although these tests were carried out under significantly different loading levels, the mechanism of crack initiation is similar. The process of cracking has started from the surface and propagated into the material. Magnified pictures placed on the right side indicate that there are numerous origins caused simultaneously by crack development in many places. The initiation of fatigue cracks proceeded in local strains and stress concentrations within the rolled-in hard and brittle scale particles the surface of the material (indicated by yellow arrows). Individual initial cracks join together into the much greater cracks which propagate into deeper parts of the material affected by fatigue.

Representative examples of fatigue fractures received from examined welded joints are presented in Figures 6(a) and 6(b). These pictures were made for the samples, both I-shaped (a) and V-shaped (b), tested at the total strain amplitude $\varepsilon_a = 0.2\%$. All received results of the study on crack initiation are similar, namely, the fractures initiated in the notch root, and in considered welded joints, they have been at the surface in the vicinity of fusion line. Detailed studies, presented in magnified pictures, have revealed that

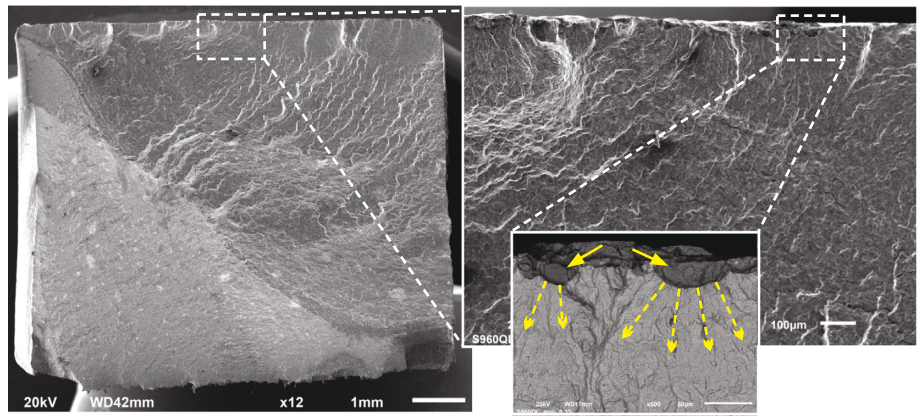

(a)

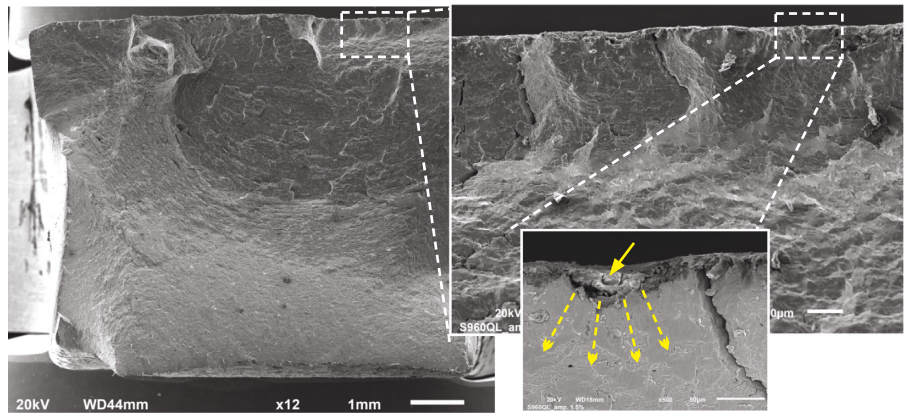

(b)

Figure 5: The pictures of fatigue fractures have been observed during fractographic investigation. Samples made of S960QL steel tested under total strain amplitude: (a) $\varepsilon_a = 0.3\%$ and (b) $\varepsilon_a = 1.5\%$.

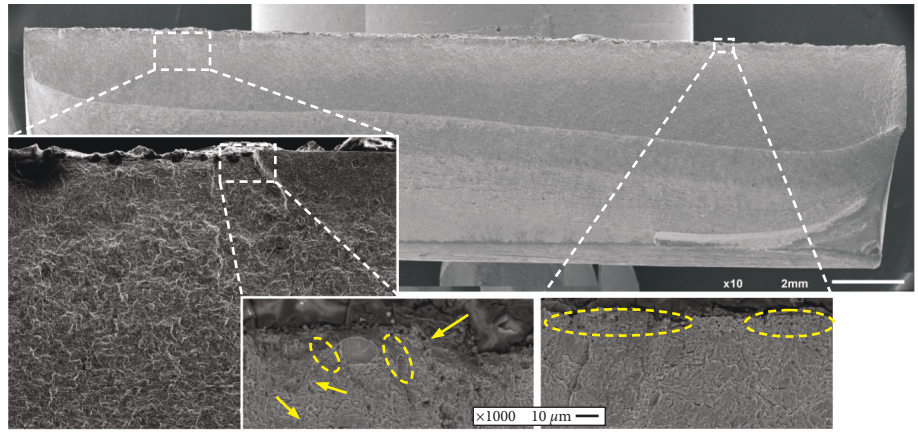

(a)

Figure 6: Continued.

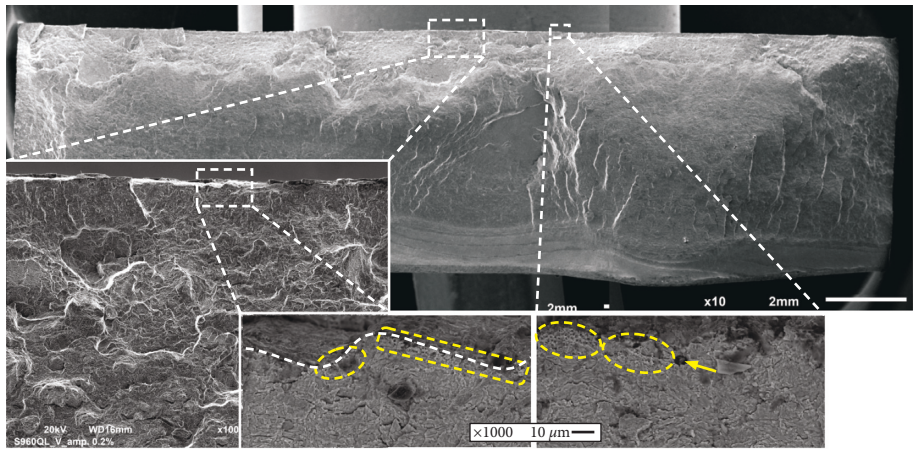

(b)

Figure 6: The pictures of fatigue fractures have been observed during fractographic investigation. Samples of weldments made of S960QL steel tested under the total strain amplitude $\varepsilon_a = 0.2\%$: (a) I-shaped and (b) V-shaped welds.

there were no dominating origins of fatigue cracks, and the initiation in both cases occurred over almost the entire length of the fusion line. It should be emphasized that the cracks in all researched V-shaped welded joints have propagated form the root side. The cracking process was probably affected by the presence of numerous micropores (surrounded regions) and inclusions, rare but existing (indicated by arrows). These imperfections in the microscale have caused local weakness of the welded material independently from the adverse microstructural changes. Moreover, the shape of the fusion line is also undesirable because it is wavy causing an additional strain concentration (Figure 6(b), the white dashed line in the nether picture).

5. Conclusions

In this paper, a method of the fatigue life prediction based on the criterion of permissible strain range in the notch root was developed. This model was verified for welded joints made of high-strength steel S960QL. Moreover, the fatigue crack initiation stage was investigated by fractographic analysis and the origins were revealed. From the obtained results and observations made, the following conclusions can be drawn:

(1) The simplified model of fatigue life prediction which was previously developed for mild and carbon steels can also be engaged for fine-grained bainitic-martensitic HSS steels.

(2) The method of fatigue life prediction based on the criterion of permissible strain range in the notch root indicates satisfactory correlation with experimental data and safely describes the fatigue life of weldments made of S960QL.

(3) The estimated limit value of the strain range in the notch root $\Delta\varepsilon_{notch}$ equals $3.11 \cdot 10^{-3}$, resulting in the stress range $\Delta\sigma$ of 300 MPa.

(4) The direct impact of the surface imperfections on the fatigue cracks initiation was revealed. In the case of paternal material, the origins of cracking were discovered at the places of rolled-in hard and brittle scale particles. In welded joints, the fatigue cracks initiated at the whole length of the fusion line.

Data Availability

The data underlying the findings of this study and other more detailed information are available from the author upon request.

Conflicts of Interest

The author declares that there are no conflicts of interest regarding the publication of this paper.

Acknowledgments

The author is grateful to Prof. Lucjan Śnieżek for advice and guidance and also to Janusz Torzewski, Ph.D., who have supported the realization of fatigue tests. The execution of fatigue tests was financially supported by the Faculty of Mechanical Engineering through the internal academic grant (RMN 08-878). The processing charge was also financed by this faculty.

References

[1] A. Hobbacher, *Recommendations for Fatigue Design of Welded Joints and Components*, International Institute of Welding, Paris, France, 2008.

[2] I. Al Zamzami and L. Susmel, "On the accuracy of nominal, structural, and local stress based approaches in designing aluminium welded joints against fatigue," *International Journal of Fatigue*, vol. 101, pp. 137–158, 2017.

[3] T. Shiozaki, N. Yamaguchi, Y. Tamai, J. Hiramoto, and K. Ogawa, "Effect of weld toe geometry on fatigue life of lap fillet welded ultra-high strength steel joints," *International Journal of Fatigue*, vol. 116, pp. 409–420, 2018.

[4] W. Hiramoto, W. Jiang, X. Zhao, and S. T. Tu, "Fatigue life of a dissimilar welded joint considering the weld residual stress:

experimental and finite element simulation," *International Journal of Fatigue*, vol. 109, pp. 182–190, 2018.

[5] C. Cui, Q. Zhang, Y. Bao, J. Kang, and Y. Bu, "Fatigue performance and evaluation of welded joints in steel bridges," *Journal of Constructional Steel Research*, vol. 148, pp. 450–456, 2018.

[6] D. Kang, C. M. Sonsino, and W. Fricke, *Fatigue Assessment of Welded Joints by Local Approaches*, Woodhead Publishing Limited, Cambridge, UK, 2007.

[7] E. Niemi, W. Fricke, and S. J. Maddox, *Fatigue Analysis of Welded Components: Designer's Guide to The Structural Hot-Spot Stress Approach*, Woodhead Publishing Limited, Cambridge, UK, 2006.

[8] L. Rong, L. Yuqing, J. Bohai, M. Wang, and Y. Tian, "Hot spot stress analysis on rib–deck welded joint in orthotropic steel decks," *Journal of Constructional Steel Research*, vol. 97, pp. 1–9, 2014.

[9] Y. Kim, J. S. Oh, and S. H. Jeon, "Novel hot spot stress calculations for welded joints using 3D solid finite elements," *Marine Structures*, vol. 44, pp. 1–18, 2015.

[10] I. A. Zamzami and L. Susmel, "On the use of hot-spot stresses, effective notch stresses and the point method to estimate lifetime of inclined welds subjected to uniaxial fatigue loading," *International Journal of Fatigue*, vol. 117, pp. 432–449, 2018.

[11] N. Osawa, N. Yamamoto, T. Fukuoka, J. Sawamura, H. Nagai, and S. Maeda, "Study on the preciseness of hot spot stress of web-stiffened cruciform welded joints derived from shell finite element analyses," *Marine Structures*, vol. 24, no. 3, pp. 207–238, 2011.

[12] M. H. Sawamura, S. M. Kim, Y. N. Kim et al., "A comparative study for the fatigue assessment of a ship structure by use of hot spot stress and structural stress approaches," *Ocean Engineering*, vol. 36, no. 14, pp. 1067–1072, 2009.

[13] C. M. Sonsino, W. Fricke, F. de Bruyne, A. Hoppe, A. Ahmadi, and G. Zhang, "Notch stress concepts for the fatigue assessment of welded joints -background and applications," *International Journal of Fatigue*, vol. 34, no. 1, pp. 2–16, 2012.

[14] T. Nykänen, H. Mettänen, T. Björk, and A. Ahola, "Fatigue assessment of welded joints under variable amplitude loading using a novel notch stress approach," *International Journal of Fatigue*, vol. 101, pp. 177–191, 2017.

[15] L. Bertini, F. Frendo, and G. Marulo, "Fatigue life assessment of welded joints by two local stress approaches: the notch stress approach and the peak stress method," *International Journal of Fatigue*, vol. 110, pp. 246–253, 2018.

[16] K. Rother and W. Fricke, "Effective notch stress approach for welds having low stress concentration," *International Journal of Pressure Vessels and Piping*, vol. 147, pp. 12–20, 2016.

[17] C. Morgenstern, C. Sonsino, A. Hobbacher, and F. Sorbo, "Fatigue design of aluminium welded joints by the local stress concep with the ficitious notch radius of r_f =1 mm," *International Journal of Fatigue*, vol. 28, no. 8, pp. 881–890, 2006.

[18] C. M. Sorbo, "A consideration of allowable equivalent stresses for fatigue design of welded joints according to the notch stress concept with the reference radii r_{ref} =1.00 and 0.05 mm," *Welding in the World*, vol. 53, no. 3-4, pp. R64–R75, 2009.

[19] R. Sołtysiak and D. Boroński, "Strain analysis at notch root in laser welded samples using material properties of individual weld zones," *International Journal of Fatigue*, vol. 74, pp. 71–80, 2015.

[20] D. Radaj, "Review of fatigue strength assessment of non-welded and welded structures based on local parameters," *International Journal of Fatigue*, vol. 18, no. 3, pp. 153–170, 1996.

[21] S. S. Manson, *Fatigue: a Complex Subject-Some Simple Approximations*, NASA, Washington, DC, USA, 1965.

[22] S. Kocańda and A. Kocańda, *Niskocyklowa Wytrzymałość Zmęczeniowa Metali*, in Polish, PWN, Warszawa, Poland, 1989.

[23] C. Goss, S. Kłysz, and W. Wojnowski, *Problemy Niskocyklowej Trwałości Zmęczeniowej Wybranych Stali I Połączeń Spawanych*, in Polish, Wydawnictwo ITWL, Warszawa, Poland, 2004.

[24] N. A. Machutow, A. P. Gusienkow, and M. M. Galenin, *Rasczjoty Prochnosti Elementow Konstrukcijj Pri Malocyklowom Nagruzhenii*, in Russian, Metodicheskie ukazania, Moscow, Russia, 1987.

[25] ISO 6892-1: Metallic Materials–Tensile Testing–Part 1: Method of Test at Room Temperature.

[26] ASTM E 606-04, *Standard Practice for Strain-Controlled Fatigue Testing*, ASTM, West Conshohocken, PA, USA, 2005.

[27] K. Ida and T. Uemura, "Stress concentration factor formulae widely used in Japan," *Fatigue & Fracture of Engineering Materials and Structures*, vol. 19, no. 6, pp. 779–786, 1996.